Dalton Transactions

ARTICLE

Giant negative magnetoresistance effect in an iron tetrabenzoporphyrin complex

Received 00th January 20xx,
Accepted 00th January 20xx

DOI: 10.1039/x0xx00000x

www.rsc.org/

Miki Nishi,[a] Mitsuo Ikeda,[b] Akinori Kanda,[b] Noriaki Hanasaki,[b] Norihisa Hoshino,[c] Tomoyuki Akutagawa,[c] and Masaki Matsuda[a*]

By measuring the electrical resistivity in TPP[Fe^{III}(tbp)$(CN)_2$]$_2$ (TPP = tetraphenylphosphonium and tbp = tetrabenzoporphyrin) under the application of a static magnetic field, the giant negative magnetoresistance (MR) effect with high anisotropy is observed. More specifically, the MR ratio at 13 K under a field of 9 T perpendicular to the *c* axis is −70%, whereas the MR ratio under a field parallel to the *c* axis is −40%. Furthermore, electron spin resonance (ESR) measurements indicate large anisotropy in the principal *g*-values of d spin (S = 1/2) in the [Fe^{III}(tbp)$(CN)_2$] unit; the g_1 value almost perpendicular to the tbp plane and the g_2 and g_3 values almost parallel to the tbp plane are 3.60, 1.24, and 0.39, respectively. It is revealed that the anisotropy in the MR effect arises from the anisotropy in d spin, suggesting that the d spins in TPP[Fe^{III}(tbp)$(CN)_2$]$_2$ affect the π-conduction electron via the intramolecular π-d interaction. The anisotropy and magnitude in the giant negative MR effect for TPP[Fe^{III}(tbp)$(CN)_2$]$_2$ are smaller than the corresponding values for the isostructural phthalocyanine (Pc) analogue TPP[Fe^{III}(Pc)$(CN)_2$]$_2$. This is consistent with the fact that the intermolecular antiferromagnetic d–d interaction in TPP[Fe^{III}(tbp)$(CN)_2$]$_2$ (suggested by the Weiss temperature: Θ = −8.0 K) is weaker than that in TPP[Fe^{III}(Pc)$(CN)_2$]$_2$ (Θ = −12.3 K). This indicates that the minor modification in coordination complexes can significantly affect the MR effect via tuning the intermolecular d–d interaction as well as the intermolecular π–π overlap.

Introduction

The study of spintronics, in which both the electronic and magnetic natures of the electron are utilized as charge and spin, has attracted significant interest in device applications because of the value of emerging phenomena such as the giant magnetoresistance (MR) effect or spin-polarized electron injection. Various devices based on the development of spintronics have become indispensable in modern technology.[1, 2] More specifically, a typical system of compounds that exhibit the giant MR effect is the family of perovskite manganese oxides, whose MR effect arises from the interaction between the conduction electron's spin in the e_g orbital and localized spins in the t_{2g} orbitals.[3, 4]

Recently, by applying a similar concept to perovskite manganese oxides in the context of molecular compounds, the development of molecular spintronic devices that exhibit the giant MR effect has been attempted. The most successful report is the molecular conductor λ-$(BETS)_2FeCl_4$ (BETS = bis(ethylenedithio)-tetraselenafulvalene), which shows a field-induced superconducting state derived from the interaction between the spin of the π–conduction electron and d–localized spin (π–d interaction).[5, 6] Up to the present, various molecular conductors with a magnetic species as a counter ion have been reported.[7–9] However, it is difficult to establish a molecular design that yields the giant MR effect with certainty. This is because the strong π–d interaction related to the positions of both the π–conduction electron and d–localized spin in the crystal structure cannot be guaranteed by merely ensuring that the system contains both of them.

Meanwhile, we have considered coordination complexes as a fruitful component for constructing molecular spintronic devices; that is because they can have both π–conduction electrons and d spin in a ligand and a ligated metal ion, respectively. Among them, we have focused on phthalocyanine (Pc), a π–conjugated macrocyclic ligand, and constructed molecular conductors using a [Fe^{III}(Pc)$(CN)_2$] unit; in this unit, the d spin (S = 1/2) in the central iron(III) ion, which exists on degenerated d_{xz} and d_{yz} orbitals, is surrounded by π delocalized electrons of Pc.[10] In the [Fe^{III}(Pc)$(CN)_2$] unit, the highest occupied molecular orbital (HOMO) consists of the π orbital of Pc, and the next HOMOs reflect the d_{xz} and d_{yz} orbitals of the iron(III) ion.[11, 12] As a result, this induces the strong π–d interaction in the molecular unit itself, irrespective of the crystal structure.[13] Therefore, all of the molecular conductors composed of the [Fe^{III}(Pc)$(CN)_2$] unit exhibit the giant negative MR effect, which originates from the strong π–d interaction.[13–15] The MR ratio, which is defined as $\Delta\rho(B)/\rho(0)$ =

[a] Department of Chemistry, Kumamoto University, 2-39-1 Kurokami, Chuo-ku, Kumamoto 860-8555, Japan. E-mail: masaki@sci.kumamoto-u.ac.jp
[b] Department of Physics, Osaka University, 1-1 Machikaneyama, Toyonaka 560-0043, Japan.
[c] Institute of Multidisciplinary Research for Advanced Materials, Tohoku University, 2-1-1 Katahira Sendai 980-8577, Japan.

†Electronic Supplementary Information (ESI) available: crystallographic data in CIF for PNP[Fe^{III}(tbp)$(CN)_2$] see DOI: 10.1039/x0xx00000x

($\rho(B)$–$\rho(0)$)/$\rho(0)$, where $\rho(B)$ represents electrical resistivity under a magnetic field, reaches −99% under a 42 T magnetic field for TPP[Fe^{III}(Pc)$(CN)_2]_2$ (TPP = tetraphenylphosphonium).

As for TPP[Fe^{III}(Pc)$(CN)_2]_2$, the 1:2 ratio of cation:[Fe^{III}(Pc)$(CN)_2$] units gives an effective charge of −0.5 for one [Fe^{III}(Pc)$(CN)_2$] unit; each Pc ring is formally oxidized by 0.5e from the initial closed-shell Pc^{2-}. Crystal structure analysis reveals that the [Fe^{III}(Pc)$(CN)_2$] unit uniformly stacks along the *c* axis. Therefore, TPP[Fe^{III}(Pc)$(CN)_2]_2$ forms a one-dimensional 3/4-filled π–orbital based HOMO band.[10] However, in spite of the 3/4-filled HOMO band, TPP[Fe^{III}(Pc)$(CN)_2]_2$ exhibits semiconducting behaviour owing to the fluctuation of the charge ordering state of π electrons, which is ascertained by nuclear quadrupole resonance (NQR) measurements for isostructural TPP[Co^{III}(Pc)$(CN)_2]_2$, where the central cobalt(III) ion is non-magnetic.[16] In the 3/4-filled π–system, it is theoretically predicted that the introduction of the antiferromagnetic ordered localized d spins stabilizes the charge ordering state of π electrons via the π–d interaction.[17, 18] In fact, the antiferromagnetic ordering of d spins in TPP[Fe^{III}(Pc)$(CN)_2]_2$ was observed by a magnetic torque study.[19] Therefore, the charge ordering state of π electrons in TPP[Fe^{III}(Pc)$(CN)_2]_2$ is believed to be enhanced compared to that of the non-magnetic cobalt(III) system. Furthermore, the suppression of the ordering state of π electrons by an external magnetic field has also been reported.[19] Therefore, it is believed that the origin of the giant negative MR effect in TPP[Fe^{III}(Pc)$(CN)_2]_2$ is the suppression of the charge ordering state of π electrons by the external magnetic field, which is enhanced by the intermolecular antiferromagnetic d–d interaction via the intramolecular π–d interaction. A similar giant negative MR effect could be observed in various $[Cat]_x[M^{III}(Pc)L_2]_y$ systems, where Cat represents a cationic component, M represents Fe or Cr, and L represents CN, Cl or Br.[14, 15, 20–23] This would mean that M(Pc) is an ideal coordination complex for the study of molecular spintronics.

Recently, we have succeeded in fabricating the molecular conductor TPP[Fe^{III}(tbp)$(CN)_2]_2$, whose macrocyclic ligand is tetrabenzoporphyrin (tbp).[24] Because the molecular structures of tbp and Pc only differ by the atoms at four *meso* positions bridging four pyrrole units, the crystal structure of TPP[Fe^{III}(tbp)$(CN)_2]_2$ with tetragonal space group $P4_2/n$, as shown in Figure 1, is isostructural to that of TPP[Fe^{III}(Pc)$(CN)_2]_2$. However, this slight change in molecular structure induces a considerable difference in the intermolecular π–π overlap; the smaller overlap integral between the adjacent units along the *c* axis was found for TPP[Fe^{III}(tbp)$(CN)_2]_2$.[24] Since it is believed that the intermolecular antiferromagnetic d–d interaction is mediated by π electrons, the reduction in the intermolecular π–π overlap implies that the intermolecular d–d interaction is weakened.

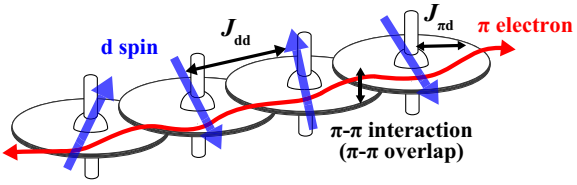

Scheme 1. The intermolecular d-d interaction (J_{dd}), intramolecular π–d interaction ($J_{\pi d}$), and intermolecular π–π interaction (π–π overlap) in a molecular conductor composed of the [Fe^{III}(Pc)$(CN)_2$] unit.

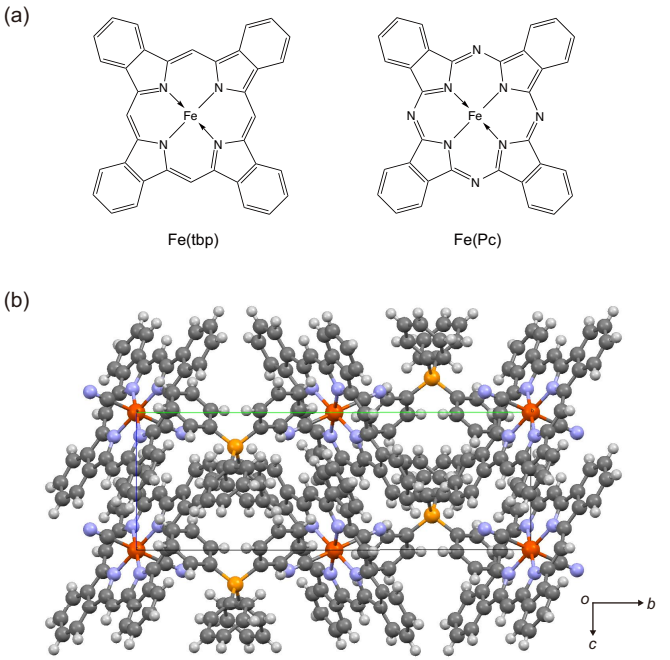

Figure 1. (a) Molecular structure of Fe(tbp) and Fe(Pc). (b) Crystal structure of TPP[Fe^{III}(tbp)$(CN)_2]_2$; view along the *a* axis. Some molecules are omitted for clarity.

In this study, by focusing our attention on the intermolecular d–d interaction, we report on the MR effect for TPP[Fe^{III}(tbp)$(CN)_2]_2$ as well as its electrical and magnetic properties. Additionally, by comparing the MR effect to that for TPP[Fe^{III}(Pc)$(CN)_2]_2$, we discuss the effect of the molecular structural change in the macrocyclic ligand on the giant MR effect.

Results and discussion

Electrical resistivity measurements

Figure 2 shows the temperature dependence of the electrical resistivity along the *c* axis of TPP[Fe^{III}(tbp)$(CN)_2]_2$ along with that of TPP[Fe^{III}(Pc)$(CN)_2]_2$. Similar to TPP[Fe^{III}(Pc)$(CN)_2]_2$, in spite of the expected 3/4-filled HOMO band, the semiconducting behaviour caused by the fluctuation of charge order was observed in the measured temperature range (i.e. 11–300 K). The inset of Figure 2 shows the Arrhenius plot of the resistivity. The activation energy for TPP[Fe^{III}(tbp)$(CN)_2]_2$ was estimated to be 0.026 eV over the entire temperature

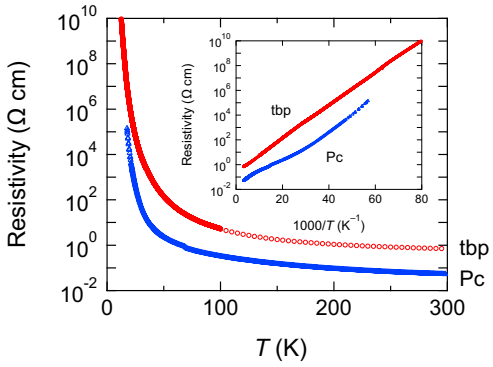

Figure 2. Temperature dependence of the electrical resistivity for TPP[Fe^{III}(tbp)$(CN)_2$]$_2$ along the *c* axis (red circles), along with that of TPP[Fe^{III}(Pc)$(CN)_2$]$_2$ (blue circles). Inset shows the Arrhenius plot.

range. Obviously, the resistivity and activation energy of TPP[Fe^{III}(tbp)$(CN)_2$]$_2$ in the high-temperature region were higher than those of TPP[Fe^{III}(Pc)$(CN)_2$]$_2$. However, TPP[Fe^{III}(tbp)$(CN)_2$]$_2$ has no inflection point where the activation energy changes, while the activation energy of TPP[Fe^{III}(Pc)$(CN)_2$]$_2$ increases around 50 K as the temperature decreases.[10] Consequently, below 50 K, the activation energy of TPP[Fe^{III}(tbp)$(CN)_2$]$_2$ becomes smaller than that of TPP[Fe^{III}(Pc)$(CN)_2$]$_2$. Because TPP[Fe^{III}(Pc)$(CN)_2$]$_2$ exhibits the giant negative MR effect below 50 K,[11] it is suggested that the inflection point observed in TPP[Fe^{III}(Pc)$(CN)_2$]$_2$ reflects the intermolecular antiferromagnetic interaction between localized d spins. Therefore, the lack of inflection point in the Arrhenius plot for TPP[Fe^{III}(tbp)$(CN)_2$]$_2$ implies a weaker antiferromagnetic d–d interaction and a smaller magnetoresitance effect compared to the case of TPP[Fe^{III}(Pc)$(CN)_2$]$_2$.

Magnetic susceptibility

Figure 3 shows the temperature dependence of the magnetic susceptibility (χ_p) of TPP[Fe^{III}(tbp)$(CN)_2$]$_2$ measured under a 1 T static magnetic field. In the high-temperature region above 20 K, the χ_p vs. *T* plot obeys the Curie-Weiss law with a Curie constant of C = 1.59 emu K mol^{-1} and a Weiss temperature of Θ = −8.0 K. Under the assumption that S = 1/2 and g = 2 for all localized spins in TPP[Fe^{III}(tbp)$(CN)_2$]$_2$, C is expected to be 1.125 or 0.750 emu K mol^{-1} for the case in which the π electron spin also behaves or does not behave as localized spin. In either case, the observed C is considerably larger than the expected value.

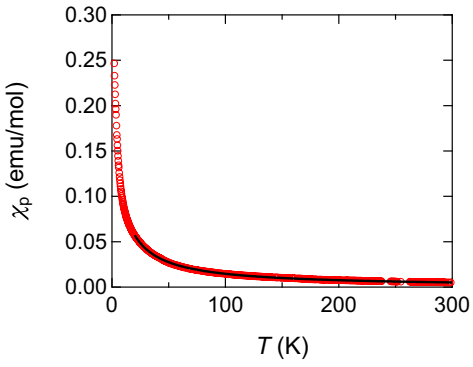

Figure 3. Temperature dependence of the magnetic susceptibility for formula unit TPP[Fe^{III}(tbp)$(CN)_2$]$_2$ under a static magnetic field of 1 T. The solid line is the best fit to the Curie-Weiss law with the parameters C = 1.59 emu K mol^{-1} and Θ = −8.0 K.

This discrepancy can be ascribed to the large anisotropic nature of the Fe^{III}-d spin in the [Fe^{III}(tbp)$(CN)_2$] unit (vide infra). The measured samples were single crystals and not orientated; however, their *c* axes were almost aligned perpendicular to the magnetic field because tiny needle crystals, whose long dimension is along the *c* axis, lay in closed-tube parallel to the magnetic field. Considering this situation along with the large *g*-value anisotropy of the Fe^{III}-d spin, the observed large Curie constant is acceptable, and a similar large value was also reported for TPP[Fe^{III}(Pc)$(CN)_2$]$_2$.[10] As for the Weiss temperature of Θ = −8.0 K, the $|\Theta|$ value is smaller than Θ = −12.3 K for TPP[Fe^{III}(Pc)$(CN)_2$]$_2$, signifying that a change in the macrocyclic ligand from Pc to tbp weakens the antiferromagnetic interaction between d spins. As a result, in the χ_p vs. *T* plot, an anomaly caused by the strong antiferromagnetic interaction was not observed for TPP[Fe^{III}(tbp)$(CN)_2$]$_2$, whereas a clear anomaly was observed around 20 K for TPP[Fe^{III}(Pc)$(CN)_2$]$_2$.[10, 19] The disappearance of the anomaly under the static 1 T magnetic field was also reported for TPP[Fe^{III}(Pc)Br_2]$_2$ and TPP[Fe^{III}(Pc)Cl_2]$_2$, whose $|\Theta|$ values are quite small compared to that of TPP[Fe^{III}(Pc)$(CN)_2$]$_2$.[20]

Magnetoresistance measurements

Figure 4(a) shows the temperature dependence of the electrical resistivity under a 9 T magnetic field perpendicular and parallel to the *c* axis, along with that under a zero magnetic field. Below around 30 K, the resistivity of TPP[Fe^{III}(tbp)$(CN)_2$]$_2$ under the magnetic field becomes smaller than that under a zero magnetic field, and the negative MR effect for the magnetic field perpendicular to the *c* axis is larger than that for the magnetic field parallel to the *c* axis. Thus, there is anisotropy in the giant negative MR effect. The magnetic field dependence of the MR effect under the field perpendicular and parallel to the *c* axis at various temperatures is shown in Figures 4(b) and (c), respectively. The negative MR effect increased upon increasing the magnetic field. As the temperature decreased or the magnetic field increased, the anisotropy and the MR effect increased. At 13 K, the resistivity under the 9 T magnetic field perpendicular to the *c* axis became 30% of that under zero magnetic field, meaning that the MR ratio under 9 T perpendicular to the *c* axis is −70%. In the giant negative MR effect, no phase transition such as insulator-metal transition was observed.

Comparing the MR effect at 20 K for TPP[Fe^{III}(tbp)$(CN)_2$]$_2$ with that for TPP[Fe^{III}(Pc)$(CN)_2$]$_2$, the MR ratios under the 9 T magnetic field perpendicular and parallel to the *c* axis of

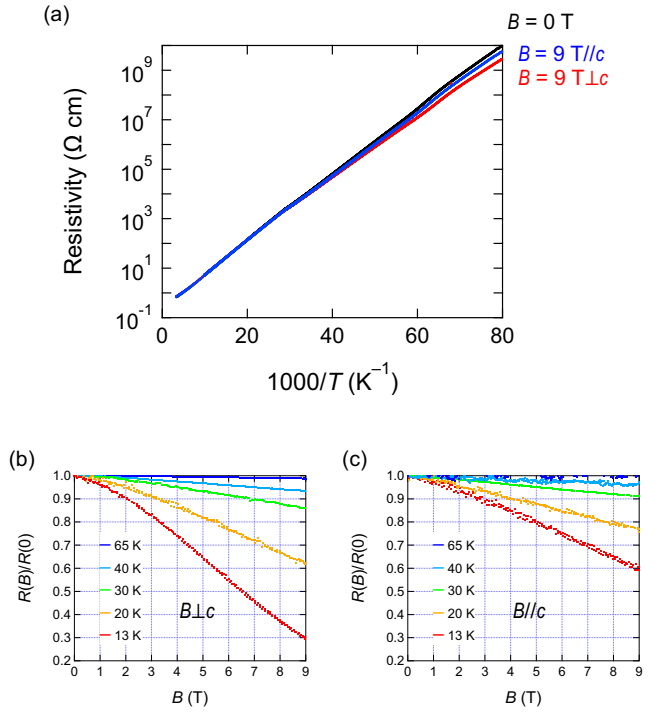

Figure 4. (a) Arrhenius plot of the electrical resistivity for TPP[Fe^{III}(tbp)(CN)$_2$]$_2$ under a zero magnetic field and static magnetic field of 9 T parallel and perpendicular to the *c* axis. Magnetic field dependence of the resistance of TPP[Fe^{III}(tbp)(CN)$_2$]$_2$ at various temperatures. (b) and (c) show the resistance normalized by that under a zero magnetic field. The resistance under the magnetic field (b) perpendicular and (c) parallel to the *c* axis.

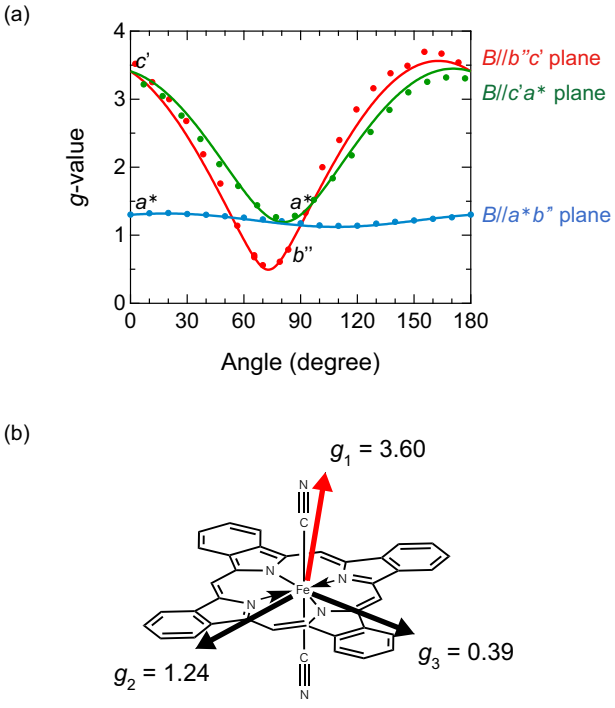

Figure 5. (a) Angular dependence of *g*-value of PNP[Fe^{III}(tbp)(CN)$_2$]. *c'* denotes the axis almost parallel to [0 1 –1], and *b''* is normal to *a** and *c'*. The solid lines are the best fit to the model for the angular dependence of the *g*-value in the orthogonal planes.[25] (b) Estimated principal *g*-values of d spin (*S* =1/2) in the [Fe^{III}(tbp)(CN)$_2$] unit.

TPP[Fe^{III}(tbp)(CN)$_2$]$_2$ are −40% and −20%, respectively, while those of TPP[Fe^{III}(Pc)(CN)$_2$]$_2$ are −70% and −30%. Therefore, it is obvious that the larger MR effect is similarly observed under the magnetic field perpendicular to the *c* axis, and that the MR ratio was smaller for TPP[Fe^{III}(tbp)(CN)$_2$]$_2$ than TPP[Fe^{III}(Pc)(CN)$_2$]$_2$, in both cases (i.e. with the magnetic field perpendicular and parallel to the *c* axis).

To investigate the magnetic nature of Fe^{III}-d spin in the [Fe^{III}(tbp)(CN)$_2$] molecular unit, electron spin resonance (ESR) measurements were performed using a single crystal of the simple salt PNP[Fe^{III}(tbp)(CN)$_2$], where PNP is bis(triphenylphosphine)iminium. In PNP[Fe^{III}(tbp)(CN)$_2$], the radical species are only the d spin of Fe^{III} (*S* = 1/2); furthermore, there is no π radical because the tbp ligand is not oxidized. Figure 5(a) shows the angular dependence of the *g*-value obtained by rotating the single crystal around the three orthogonal axes *a**, *c'*, and *b''*, where *c'* is roughly parallel to [0 1 –1], and *b''* is normal to *a** and *c'*. By fitting the experimental data to the model for the angular dependence of the *g*-value in the orthogonal planes,[25] the principal *g*-values were estimated to be g_1 = 3.60, g_2 = 1.24, and g_3 = 0.39. The principal axis of g_1 is almost parallel to the CN axis, and g_2 and g_3 are almost parallel to the tbp plane, as shown in Figure 5(b).

In the TPP[Fe^{III}(tbp)(CN)$_2$]$_2$ conductor, considering the fact that the inclinations of the CN ligand to the *c* axis and *ab* plane are 68.52° and 21.48°, respectively,[24] a larger magnetic moment is expected to occur under the magnetic field perpendicular (rather than parallel) to the *c* axis. The *g*-value anisotropy corresponds well to the anisotropy in the magnetoresistance, suggesting that d spins in TPP[Fe^{III}(tbp)(CN)$_2$]$_2$ significantly affect the π-conduction electrons via the intramolecular π-d interaction. The observed large *g*-value anisotropy is similar to that in the [Fe(Pc)(CN)$_2$] molecular unit.[12] However, the magnitude of the anisotropy in the MR effect for TPP[Fe^{III}(tbp)(CN)$_2$]$_2$ is smaller than that for TPP[Fe^{III}(Pc)(CN)$_2$]$_2$, in spite of the same molecular orientation for both TPP[Fe^{III}(tbp)(CN)$_2$]$_2$ and TPP[Fe^{III}(Pc)(CN)$_2$]$_2$. This suggests that the anisotropy in the MR effect is not only caused by the anisotropy in the *g*-values of d spin.

Table 1 summarizes the π–π overlap, d–d interaction and MR effect for TPP[Fe^{III}(tbp)(CN)$_2$]$_2$ and TPP[Fe^{III}(Pc)(CN)$_2$]$_2$. As mentioned above, the giant negative MR effect emerges because the magnetic field breaks the charge order state of π–conduction electrons developed by the antiferromagnetic interaction between localized d spins. Since the distance between d spins – i.e. the length of the *c* axis – is more than 7 Å, it is believed that the antiferromagnetic interaction should not be induced by the direct overlap of d orbitals, but is instead mediated by π electrons. Therefore, the decrease in the π–π overlap weakens the antiferromagnetic interaction, as

Table 1. Comparison of the overlap integral (s), Weiss temperature (Θ), and MR effect between TPP[Fe^{III}(tbp)$(CN)_2]_2$ and TPP[Fe^{III}(Pc)$(CN)_2]_2$. s and Θ are indices of the π–π overlap and d–d interaction, respectively.

	TPP[Fe(tbp)$(CN)_2]_2$	TPP[Fe(Pc)$(CN)_2]_2$
s ($\times 10^{-3}$) at 120 K (π–π overlap)	8.4	9.7
Θ (K) (d–d interaction)	–8.0	–12.3
MR effect at 20 K	–40%	–70%

suggested by the observed smaller $|\Theta|$ value of TPP[Fe^{III}(tbp)$(CN)_2]_2$. As a result, compared to the case of TPP[Fe^{III}(Pc)$(CN)_2]_2$, the stabilizing of the charge order state of π–conduction electrons scarcely occurs in TPP[Fe^{III}(tbp)$(CN)_2]_2$, resulting in the reduction of the negative MR effect, which originates from the break of the charge order state by the external magnetic field.

Although the details of the intramolecular π–d interaction in the [Fe^{III}(tbp)$(CN)_2$] unit remain an open issue at the present stage, we mention it here because the d–d interaction should depend not only on the intermolecular π–π overlap, but also on the intramolecular π–d interaction. It is worth noting that smaller anisotropy in the magnetic susceptibility and MR effect are observed in TPP[Fe^{III}(Pc)$Cl_2]_2$ and TPP[Fe^{III}(Pc)$Br_2]_2$ compared to TPP[Fe^{III}(Pc)$(CN)_2]_2$, despite the identical anisotropy in the g-values of the d spin and the molecular orientation for all TPP[Fe^{III}(Pc)$L_2]_2$ compounds.[21] This situation is quite similar to the case of TPP[Fe^{III}(tbp)$(CN)_2]_2$. As for the [Fe^{III}(Pc)Cl_2] and [Fe^{III}(Pc)Br_2] units, it is theoretically demonstrated that the intramolecular π-d interaction is weaker than that in the [Fe^{III}(Pc)$(CN)_2$] unit,[20] suggesting that the weaker π–d interaction induces the weaker d–d interaction as well as the smaller magnetic anisotropy. Therefore, it is believed that the π–d interaction in the [Fe^{III}(tbp)$(CN)_2$] unit is also weaker than that in the [Fe^{III}(Pc)$(CN)_2$] unit. In order to clarify the details of the π–d interaction in the [Fe^{III}(tbp)$(CN)_2$] unit, theoretical calculations and experimental estimations (as performed for TPP[Fe^{III}(Pc)$(CN)_2]_2$[20, 26]) are now in progress.

Conclusions

TPP[Fe^{III}(tbp)$(CN)_2]_2$ exhibited the anisotropic giant negative MR effect with high anisotropy, where the MR ratios under a field of 9 T perpendicular and parallel to the c axis at 13 K were −70% and −40%, respectively. The ESR measurement revealed that the anisotropy arose from the large anisotropy in the principal g-value in the [Fe^{III}(tbp)$(CN)_2$] unit; the g_1 value almost perpendicular to the tbp plane, along with the g_2 and g_3 values almost parallel to the tbp plane, were 3.60, 1.24, and 0.39, respectively. In spite of the similarity in the molecular and crystal structures and anisotropy in the principal g-values in the [Fe^{III}(tbp)$(CN)_2$] unit (compared to the [Fe^{III}(Pc)$(CN)_2$] unit), the anisotropy and magnitude in the giant negative MR effect for TPP[Fe^{III}(tbp)$(CN)_2]_2$ are smaller than those for TPP[Fe^{III}(Pc)$(CN)_2]_2$. This is consistent with the weaker intermolecular antiferromagnetic d–d interaction in TPP[Fe^{III}(tbp)$(CN)_2]_2$ (Θ = –8.0 K) compared to that in TPP[Fe^{III}(Pc)$(CN)_2]_2$ (Θ = –12.3 K), because the antiferromagnetic interaction is a principal factor in the giant negative MR effect.

This study reveals that the MR effect in coordination compounds can be precisely controlled by tuning the intermolecular π–π overlap and d-d interaction via molecular design. In the Fe^{III}(Mc)L_2-based conductors, where Mc represents a macrocyclic ligand (such as tbp or Pc), larger π–π overlap and stronger d–d interaction are preferred for the giant negative MR effect. Preliminary studies on TPP[M^{III}(tbp)$L_2]_2$ (M = Co or Fe; L = Cl or Br) conductors show the axial-ligand dependence of the π–π overlap, which differs from that in TPP[M^{III}(Pc)$L_2]_2$; the strongest π–π overlap occurs in TPP[M^{III}(tbp)$Br_2]_2$. Systematic studies for TPP[M^{III}(tbp)$L_2]_2$ and TPP[M^{III}(Pc)$L_2]_2$ (L = CN, Cl, and Br) will clarify the details of the mechanism of the giant negative MR effect in Fe^{III}(Mc)L_2-based conductors, leading to the development of molecular spintronic devices based on coordination compounds.

Experimental

Synthetic procedures

Fe(tbp) and TPP[Fe^{III}(tbp)$(CN)_2]_2$. Fe(tbp) and needle-shaped single crystals of TPP[Fe^{III}(tbp)$(CN)_2]_2$ (TPP = tetraphenylphosphonium) were fabricated by the procedure described in a previous study.[24]

PNP[Fe^{III}(tbp)$(CN)_2$]. Fe(tbp) was refluxed with an excess amount of KCN in ethanol overnight, leading to K_2[Fe^{II}(tbp)$(CN)_2$]. The cation exchange by the metathesis using bis(triphenylphosphine)iminium (PNP) iodide yielded (PNP)$_2$[Fe^{II}(tbp)$(CN)_2$]. During the recrystallization using acetonitrile under ambient conditions, (PNP)$_2$[Fe^{II}(tbp)$(CN)_2$] was air-oxidized to PNP[Fe^{III}(tbp)$(CN)_2$], and single crystals of PNP[Fe^{III}(tbp)$(CN)_2$] were obtained.

Crystal structure determination

Crystal data for PNP[Fe^{III}(tbp)$(CN)_2$] were collected at 296 K using a VariMax RAPID FR-E diffractometer with monochromated Mo-Kα radiation (λ = 0.71075 Å). The structure was solved using a direct method using SIR2004[27] and refined by a full-matrix least-squares technique with SHELXL-97[28] with anisotropic and isotropic thermal parameters for non-hydrogen and hydrogen atoms, respectively. The crystallographic data have been deposited at the Cambridge Crystallographic Data Centre (CCDC) as CCDC-1479238.

Measurements

The resistivity measurements along the c axis of a TPP[Fe^{III}(tbp)$(CN)_2]_2$ single crystal were performed using a Quantum Design PPMS with the application of the static magnetic field up to 9 T over the temperature range 11–300 K. Gold wires were attached to the sample using gold paste after gold deposition. In the high-temperature region, where the resistance was below 10^7 Ω, the standard four-probe method was adopted; in the low–temperature region, where the

resistance was above 10^6 Ω, the two-probe method was applied. The static magnetic susceptibility measurements using single crystals were performed by a Quantum Design MPMS SQUID susceptometer with a 1 T magnetic field over the temperature range of 2–300 K. The angular dependencies of the *g*-value in the ESR spectra for PNP[Fe^{III}(tbp)$(CN)_2$] at around 7 K were measured using a JEOL X-band spectrometer JES-FA200.

Acknowledgements

The authors thank Dr. Y. Hirao (Osaka University) for his help in the ESR measurement. This study was supported in part by a Grant-in-Aid for Scientific Research (C) (No. 25410097) from the Japan Society for the Promotion of Science.

Notes and references

1 I. Žutić, J. Fabian and S. D. Sarma, *Rev. Mod. Phys.*, 2004, **76**, 323.
2 S. A. Wolf, D. D. Awschalom, R. A. Buhrman, J. M. Daughton, S. von Molnár, M. L. Roukes, A. Y. Chtchelkanova and D. M. Treger, *Science*, 2001, **294**, 1488.
3 A. Urushibara, Y. Moritomo, T. Arima, A. Asamitsu, G. Kido and Y. Tokura, *Phys. Rev.* B, 1995, **51**, 14103.
4 H. Kuwahara, Y. Tomioka, A. Asamitsu, Y. Moritomo and Y. Tokura, *Science*, 1995, **270**, 961.
5 S. Uji, H. Shinagawa, T. Terashima, T. Yakabe, Y. Terai, M. Tokumoto, A. Kobayashi, H. Tanaka and H. Kobayashi, *Nature*, 2001, **410**, 908.
6 H. B. Cui, H. Kobayashi and A. Kobayashi, *J. Mater. Chem.*, 2007, **17**, 45.
7 E. Coronado and P. Day, *Chem. Rev.*, 2004, **104**, 5419.
8 T. Enoki and A. Miyazaki, *Chem. Rev.*, 2004, **104**, 5449.
9 T. Sugimoto, H. Fujiwara, S. Noguchi and K. Murata, *Sci. Technol. Adv. Mater.*, 2009, **10**, 024302.
10 M. Matsuda, T. Naito, T. Inabe, N. Hanasaki, H. Tajima, T. Otsuka, K. Awaga, B. Narymbetov and H. Kobayashi, *J. Mater. Chem.*, 2000, **10**, 631.
11 N. Hanasaki, H. Tajima, M. Matsuda, T. Naito and T. Inabe, *Phys. Rev.* B, 2000, **62**, 5839.
12 N. Hanasaki, M. Matsuda, H. Tajima, T. Naito and T. Inabe, *J. Phys. Soc. Jpn.*, 2003, **72**, 3226.
13 N. Hanasaki, M. Matsuda, H. Tajima, E. Ohmichi, T. Osada, T. Naito and T. Inabe, *J. Phys. Soc. Jpn.*, 2006, **75**, 033703.
14 M. Matsuda, T. Asari, T. Naito, T. Inabe, N. Hanasaki and H Tajima, *Bull. Chem. Soc. Jpn.*, 2003, **76**, 1935.
15 T. Inabe and H. Tajima, *Chem. Rev.*, 2004, **104**, 5503.
16 N. Hanasaki, K. Masuda, K. Kodama, M. Matsuda, H. Tajima, J. Yamazaki, M. Takigawa, J. Yamaura, E. Ohmichi, T. Osada, T. Naito and T. Inabe, *J. Phys. Soc. Jpn.*, 2006. **75**, 104713.
17 H. Seo, C. Hotta and H. Fukuyama, *Chem. Rev.*, 2004, **104**, 5005.
18 Y. Otsuka, H. Seo and Y. Motome, *J. Phys. Soc. Jpn.*, 2014, **83**, 083703.
19 H. Tajima, G. Yoshida, M. Matsuda, K. Nara, K. Kajita, Y. Nishio, N. Hanasaki, T. Naito and T. Inabe, *Phys. Rev.* B, 2008, **78**, 064424.
20 D. E. C. Yu, M. Matsuda, H. Tajima, A. Kikuchi, T. Taketsugu, N. Hanasaki, T. Naito and T. Inabe, *J. Mater. Chem.*, 2009, **19**, 718.
21 D. E. C. Yu, M. Matsuda, H. Tajima, T. Naito and T. Inabe, *Dalton Trans.*, 2011, **40**, 2283.
22 Y. Takita, H. Hasegawa, Y. Takahashi, J. Harada, A. Kanda, N. Hanasaki and T. Inabe, *J. Porphyrins Phthalocyanines*, 2014, **18**, 814.
23 M. Ikeda, T. Kida, T. Tahara, H. Murakawa, M. Nishi, M. Matsuda, M. Hagiwara, T. Inabe and N. Hanasaki, *J. Phys. Soc. Jpn.*, 2016, **85**, 064713.
24 M. Nishi, M. Matsuda, N. Hoshino and T. Akutagawa, *Chem. Lett.*, 2015, **44**, 390.
25 A. Carrington and A. D. McLachlan, *Introduction to Magnetic Resonance*, Harper and Row, New York (1967).
26 H. Murakawa, A. Kanda, M. Ikeda, M. Matsuda and N. Hanasaki, *Phys. Rev.* B, 2016, **92**, 054429.
27 M. C. Burla, R. Caliandro, M. Camalli, B. Carrozzini, G. L. Cascarano, L. De Caro, C. Giacovazzo, G. Polidori and R. Spagna, *J. Appl. Cryst.*, 2005, **38**, 381.
28 G. M. Sheldrick, *Acta. Cryst.* 2008, A**64**, 112.

